Front. Optoelectron. 2013, 6(4): 413–417
DOI 10.1007/s12200-013-0353-7

RESEARCH ARTICLE

High efficiency monobasal solid-state dye-sensitized solar cell with mesoporous TiO_2 beads as photoanode

Heng WANG, Peng XIANG, Mi XU, Guanghui LIU, Xiong LI, Zhiliang KU, Yaoguang RONG, Linfeng LIU, Min HU, Ying YANG, Hongwei HAN (✉)

Michael Grätzel Center for Mesoscopic Solar Cells, Wuhan National Laboratory for Optoelectronics, Huazhong University of Science and Technology, Wuhan 430074, China

Abstract A monobasal solid-state dye-sensitized solar cell (ssDSC) with mesoporous TiO_2 beads was developed and an efficiency of 4% was achieved under air mass (AM) 1.5 illumination. Scattering properties and electron diffusion coefficients of TiO_2 mesoporous beads and P25 nano-particles were investigated. The results show that TiO_2 mesoporous beads display higher scatterance than P25 nano-particles, and TiO_2 mesoporous beads have higher electron diffusion coefficients ($2.86 \times 10^{-5}\ cm^2 \cdot s^{-1}$) than P25 nano-particles ($2.26 \times 10^{-5}\ cm^2 \cdot s^{-1}$).

Keywords dye-sensitized solar cells (DSCs), mesoporous beads, scattering, electron diffusion coefficients

1 Introduction

Dye-sensitized solar cells (DSCs) have attracted significant attention as cost-effective alternatives to conventional solar cells since the first report of a highly efficient DSC [1]. Recently, DSCs based on liquid electrolyte have reached a power conversion efficiency (PCE) of 12.3% under standard AM1.5G full sunlight [2]. However, these devices are still based on volatile liquid electrolyte which suffers from the problem of leakage. Solid-state dye-sensitized solar cells (ssDSCs) that applying hole transporting materials (HTMs) instead of liquid electrolyte show potential advantage of practical application due to easier encapsulation [3–8]. Over the past decade, significant progress had been achieved for ssDSCs and the highest efficiency of over 7% was obtained based on organic small molecule spiro-OMeTAD (2,2′,7,7′-tetrakis-(N,N-di-4-methoxyphenylamino)-9,9′-spirobifluorene) as the HTM [6]. However, this efficiency for ssDSC is still much lower than that of the best DSCs with liquid electrolyte. The main reason is the incomplete light harvesting since the optimized TiO_2 film thickness is only around 2 μm for ssDSCs. To increase light absorption of thin TiO_2 film, one strategy is to develop dyes with high molar extinction coefficient which can absorb sufficient light in thin active layer [5,6]. Another strategy is to utilize more efficient photoanode which combines high surface factor for sufficient dye loading, large pores for filling of HTMs, and fast charge transport for efficient charge collection. Up to date, several novel working electrodes for HTM based on ssDSCs have been developed, such as TiO_2 nanotubes [9], nanorods [10], nanofibers [11] and nanowires [12]. However, devices using these photoanodes are still less efficient than the conventional ssDSCs based on nanoporous TiO_2 particles.

In this paper, we employ mesoporous TiO_2 beads as photoanode to fabricate monobasal ssDSCs based on spiro-OMeTAD and carbon counter electrode. The monobasal ssDSCs based on P3HT and carbon counter electrode were developed by our group previously [13]. The motivation for us to use mesoporous TiO_2 beads is based on the following considerations. First, mesoporous TiO_2 beads provides a large surface area for dye absorption [14]. Secondly, the light scattering ability of beads could further help to increase light harvesting in thin TiO_2 film [14]. Thirdly, the large pores formed between the beads should be beneficial for pore filling of the HTM [14]. By utilizing an indoline dye D102, we achieved a high efficiency of 4.0%, which is comparable to the ssDSCs based on conventional nanoporous TiO_2 particles with the same dye [5].

2 Experimental section

The device structure is schematically shown in Fig. 1. The

Received June 6, 2013; accepted August 20, 2013

E-mail: hongwei.han@mail.hust.edu.cn

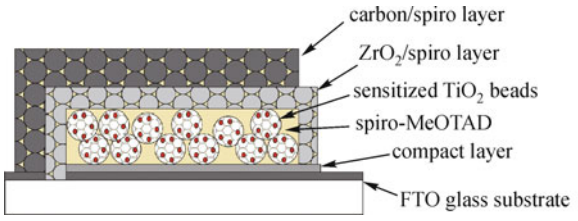

Fig. 1 Schemed structure of ssDSC based on mesoporous TiO_2 beads. Spiro-MeOTAD is filled in the pores of mesoporous TiO_2 beads layer, ZrO_2 insulating layer and carbon counter electrode layer

fluorine-doped SnO_2 substrates were etched with Zn power and HCl (1 mol/L) to form two detached electrode pattern before being ultrasonically cleaned with detergent, deionized water and ethanol respectively. After that, the patterned substrates were coated with a 100 nm compact TiO_2 layer by aerosol spray pyrolysis. Then a 2 μm mesoporous TiO_2 beads layer was deposited on top of the compact layer by screen printing. The mesoporous TiO_2 beads was synthesized with hydrothermal methods by our group previously [15]. After being sintered at 450°C for 30 min, the films were soaked in $TiCl_4$ aqueous solution (20 mmol/L) for 30 min at 70°C. The samples were sintered again at 450°C for 20 min after rinsing with deionized water. Then, a 3 μm insulating ZrO_2 layer was printed on the top of the TiO_2 beads layer by screen printing and dried at 70°C. Subsequently, a 20 μm carbon layer was deposited on the top of the ZrO_2 layer by the doctor-blade method as a counter electrode, and then the substrates were sintered at 400°C for 30 min. After cooled to 70°C, the samples were soaked in D102 solution (0.5 mmol/L in CH_3CN : t-BuOH (1:1)) overnight in the dark. After sensitization, the films were rinsed in dry ethanol for 3 times (10 min every time) and dried in air flow. Then, a chlorobenzene solution containing 0.17 mol/L spiro-MeOTAD (Merk), 0.2 mmol/L $Li(CF_3SO_2)_2N$ (Aldrich) and 0.11 mmol/L *tert*-buytlpyridine (Aldrich) was deposited onto the carbon layer. Finally, the devices were finished by drying gradually at 60°C.

The structure of mesoporous TiO_2 beads film was observed using scanning electron microscopes (SEM, FEI Sirion 200). The photocurrent density-voltage characteristics were taken with a Keithley 2400 sourcemeter under illumination with an Oriel solar simulator composed of a 1000 W xenon arc lamp and AM1.5G filters. Light intensity was calibrated with a normative silicon cell. And the test area is 0.13 cm^2. The incident photon conversion efficiency (IPCE) was measured using a 150 W xenon lamp (Oriel) fitted with a monochromator (Cornerstone 260) as a monochromatic light source. The intensity modulated photovoltage spectroscopy (IMVS)/intensity modulated photocurrent spectroscopy (IMPS) measurements were carried out using high-intensity green LEDs (530 nm) driven by a ZAHNER Xpot frequency response analyzer over a frequency range of 100 mHz to 10 kHz at a bias intensity of 0.06 sun. The LED supplied the ac (modulation depth 10%) and dc components of the illumination.

Figure 2 displays the SEM images of mesoporous TiO_2 beads film. Mesoporous TiO_2 beads were synthesized with hydrothermal method according to our previously reported paper. Large pores among beads can be clearly seen in Fig. 2(a) and this is beneficial to HTM filling. The beads size was polydisperse with diameter between 300 and 600 nm. And the beads were composed of well interconnected nanocrystals (Fig. 2(b)) with particle size of approximately 20 nm.

3 Results and discussion

For comparison, ssDSCs composed of P25 and TiO_2 beads

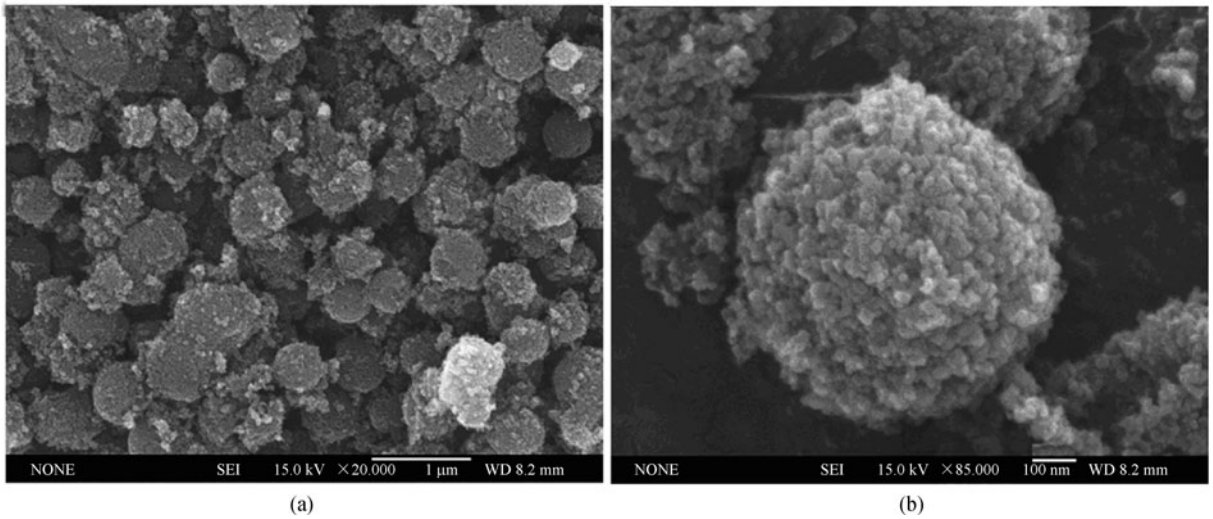

Fig. 2 Low- and high-magnification SEM images of mesoporous TiO_2 beads film. (a) Low magnification; (b) high magnification

Table 1 Summary of photovoltaic performance at an illumination intensity of one sun (AM1.5 global, 100 $mW \cdot cm^{-2}$). Devices 1 and 3 are based on P25 titania electrodes. Devices 2 and 4 are based on mesoporous TiO_2 beads electrodes. For devices 3 and 4, TiO_2 electrodes are both treated with $TiCl_4$ aqueous solution. For devices 1 and 2, TiO_2 electrodes are not treated with $TiCl_4$ aqueous solution. (J_{SC}: short circuit current density, V_{OC}: open circuit potential, *FF*: fill factor and η: conversion efficiency)

device	J_{SC}/(mA · cm^{-2})	V_{OC}/mV	*FF*	η/%
1 (P25)	3.24	785	0.49	1.24
2 (Beads)	6.72	828	0.59	3.29
3 (P25)	6.31	787	0.62	3.1
4 (Beads)	7.28	846	0.65	4.0

sensitized with D102 dye are fabricated, both before and after $TiCl_4$ post-treatment. The photovoltaic characteristics of these devices are shown in Table 1. The optimized film thicknesses of P25 and beads photoanodes are 1.7 and 1.5 μm, respectively. The best cell exhibits a short circuit current density (J_{SC}) of 7.28 mA · cm^{-2}, an open circuit voltage (V_{OC}) of 846 mV, and an efficiency of 4% for beads with $TiCl_4$ post-treatment. This performance is much better than that for P25 with $TiCl_4$ treatment (J_{SC}: 6.31 mA · cm^{-2}, V_{OC}: 787 mV, η: 3.1%). The higher J_{SC} for beads than P25 could be mainly attributed to two factors. First, beads can absorb more dye molecular than P25 for the same thickness due to larger surface area [14]. Secondly, better light scattering property for beads further increase the number of photon absorbed by dyes. We also investigated the effect of $TiCl_4$ post-treatment for the cells. With $TiCl_4$ post-treatment, devices demonstrated better performance compared to those without $TiCl_4$ post-treatment for both beads and P25. This is consistent with early reports for ssDSCs [16].

Figure 3(a) shows the photocurrent density-voltage curves of the cells based on P25 and beads with $TiCl_4$ post-treatment, at sunlight intensity of 100 mW · cm^{-2}. The external quantum efficiency of the two cells is displayed in Fig. 3(b). For beads electrode, the IPCE is superior from 400 to 600 nm, where the D102 dye absorbs efficiently. The IPCE attains a maximum of 56% at 480 nm. By contrast, the maximum IPCE of P25 titania electrode was only 43% at the same wavelength. Such an enhancement verified the increased J_{SC} for beads.

To have further understanding of the effect of different photoanodes on device performance, intensity modulated photocurrent spectroscopy (IMPS) and intensity modulated photovoltage spectroscopy (IMVS) have also been employed to investigate the charge transport and recombination characteristics in mesoporous TiO_2 beads and P25 titania-based cells. In these measurements, frequency-dependent photocurrent or photovoltage responses of a typical cell to modulated incident light were recorded. The IMPS and IMVS measurements are shown in Figs. 4(a) and 4(b) respectively. The transport time (τ_d) of injected electrons through TiO_2 film can be obtained from the equation $\tau_d = (2\pi f_{d,min})^{-1}$ [11], where $f_{d,min}$ is the

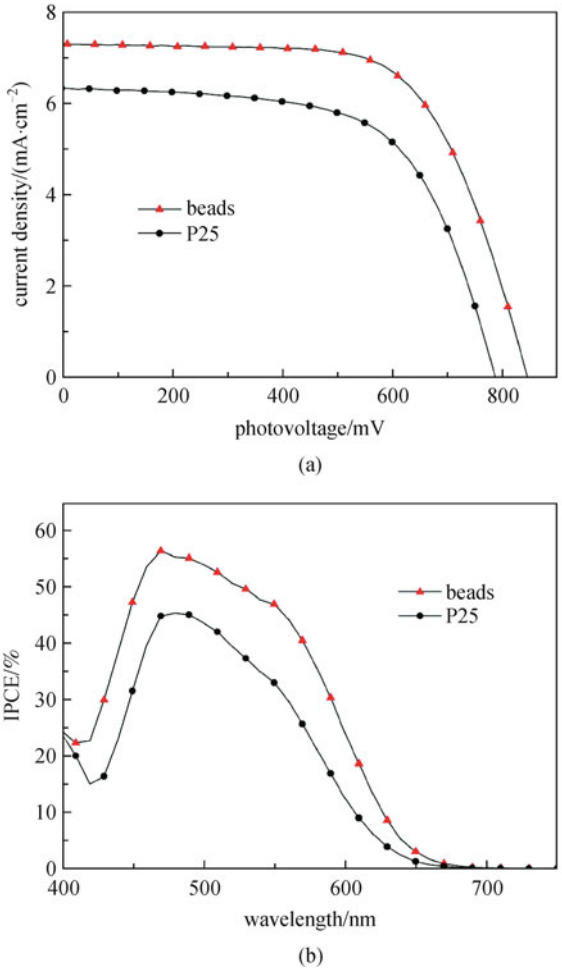

Fig. 3 Photocurrent density-voltage curves (a) and IPCE spectra (b) of ssDSCs based on mesoporous TiO_2 beads and P25 titania electrode with $TiCl_4$ treatment

characteristic frequency at the minimum of the IMPS imaginary component. Therefore, τ_d values are estimated to be 0.38 and 0.48 ms in mesoporous TiO_2 beads and P25 films, respectively. In addition, from the equation $D_n = d^2(2.35\tau_d)^{-1}$ [11], in which d is the thickness of the photoanodes (1.6 μm), the electron diffusion coefficients (D_n) in mesoporous TiO_2 beads and P25 films are

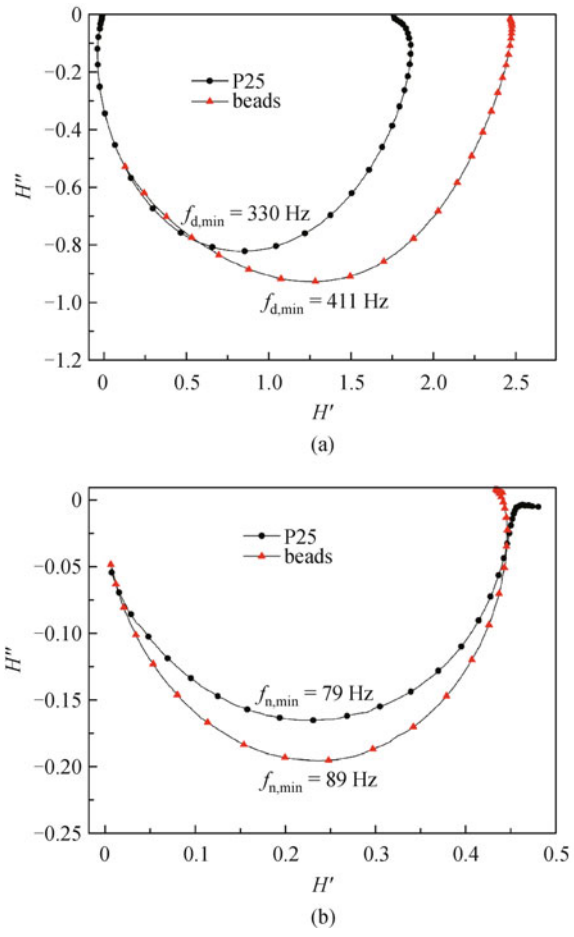

Fig. 4 IMPS (a) and IMVS (b) of ssDSCs based on mesoporous TiO_2 beads and P25 titania electrode

calculated to be 2.86×10^{-5} and 2.26×10^{-5} $cm^2 \cdot s^{-1}$, respectively. The slightly higher D_n for mesoporous TiO_2 beads film indicates that the well interconnected particles in beads could be beneficial to charge transportation.

The recombination lifetime (τ_n) was calculated using the equation $\tau_n = (2\pi f_{n,min})^{-1}$ [11], where $f_{n,min}$ is the characteristic frequency at the minimum of the IMVS imaginary component. Thus, τ_n values are estimated to be 1.79 and 2.01 ms for mesoporous TiO_2 beads and P25 films, respectively. The electron lifetime for mesoporous TiO_2 beads was a little lower than that for P25. In consideration of the larger surface area of mesoporous TiO_2 beads than P25 tiatania film, this could be attributed to that large surface area of mesoporous TiO_2 beads electrode results in large contact area between TiO_2 photoanode and HTM, and then more chance for charge recombination. However, the V_{OC} for beads based devices is around 60 mV higher than that for P25 based devices. Photovoltage is defined as the difference between the Fermi level of photoanode and the Fermi level of HTM. Because mesoporous beads electrode can absorb more dyes than P25 titania electrode with the same film thickness, more electrons are injected into mesoporous beads electrode than P25 titania electrode. Higher electron density leads to higher Fermi level for mesoporous beads electrode than P25 titania electrode and higher V_{OC}.

To further confirm the reason for improved photocurrent for beads, we investigated the charge collection efficiency (η_{mL}), which is described by the equation $\eta_{mL} = 1 - \tau_d \tau_n^{-1}$. η_{mL} for beads and P25 based devices were calculated to be 78.8% and 76.1% respectively. The similar charge collection efficiency indicates that the different photocurrent for beads and P25 was not attributed to the difference in charge collection efficiency. Consequently, the higher photocurrent for beads could mainly be resulted from the different light harvesting ability for beads and P25.

4 Conclusions

In summary, mesoporous TiO_2 beads have demonstrated great potential as photoanode in ssDSCs and an efficiency of 4% could be achieved with D102 dye. This efficiency is comparable to the ssDSCs based on conventional TiO_2 nanoparticles with the same dye [5]. Devices based on mesoporous TiO_2 beads exhibit higher J_{SC} and V_{OC} than devices based on P25 titania electrodes. The better photovoltaic performance for beads based devices is mainly due to the better light harvesting ability. Further improvements could be expected by controlling the beads size and utilizing sensitizers with broader absorption spectrum.

Acknowledgements The authors acknowledge the financial support by the National High Technology Research and Development Program of China (863) (No. SS2013AA50303), the National Natural Science Foundation of China (Grant No. 61106056), the Fundamental Research Funds for the Central Universities (HUSTNY022), and Scientific Research Foundation for Returned Scholars, Ministry of Education of China. We thank Analytical and Testing Center of Huazhong University of Science and Technology (HUST) for field emission scanning electron microscopy (FESEM) testing.

References

1. O'Regan B, Grätzel M. A low-cost, high-efficiency solar cell based on dye-sensitized colloidal TiO_2 films. Nature, 1991, 353(6346): 737–740
2. Yella A, Lee H W, Tsao H N, Yi C Y, Chandiran A K, Nazeeruddin M K, Diau E W G, Yeh C Y, Zakeeruddin S M, Grätzel M. Porphyrin-sensitized solar cells with cobalt (II/III)-based redox electrolyte exceed 12 percent efficiency. Science, 2011, 334(6056): 629–634
3. Hagen J, Schaffrath W, Otschik P, Fink R, Bacher A, Schmidt H W, Haarer D. Novel hybrid solar cells consisting of inorganic nanoparticles and an organic hole transport material. Synthetic Metals, 1997, 89(3): 215–220

4. Bach U, Lupo D, Comte P, Moser J E, Weissortel F, Salbeck J, Spreitzer H, Grätzel M. Solid-state dye-sensitized mesoporous TiO_2 solar cells with high photon-to-electron conversion efficiencies. Nature, 1998, 395(6702): 583–585
5. Schmidt-Mende L, Bach U, Humphry-Baker R, Horiuchi T, Miura H, Ito S, Uchida S, Grätzel M. Organic dye for highly efficient solid-state dye-sensitized solar cells. Advanced Materials, 2005, 17(7): 813–815
6. Burschka J, Dualeh A, Kessler F, Baranoff E, Cevey-Ha N L, Yi C Y, Nazeeruddin M K, Grätzel M. Tris(2-(1H-pyrazol-1-yl)pyridine) cobalt(III) as p-type dopant for organic semiconductors and its application in highly efficient solid-state dye-sensitized solar cells. Journal of the American Chemical Society, 2011, 133(45): 18042–18045
7. Cai N, Moon S J, Cevey-Ha L, Moehl T, Humphry-Baker R, Wang P, Zakeeruddin S M, Grätzel M. An organic D-π-A dye for record efficiency solid-state sensitized heterojunction solar cells. Nano Letters, 2011, 11(4): 1452–1456
8. Snaith H J, Moule A J, Klein C, Meerholz K, Friend R H, Grätzel M. Efficiency enhancements in solid-state hybrid solar cells via reduced charge recombination and increased light capture. Nano Letters, 2007, 7(11): 3372–3376
9. Mor G K, Kim S, Paulose M, Varghese O K, Shankar K, Basham J, Grimes C A. Visible to near-infrared light harvesting in TiO_2 nanotube array-P3HT based heterojunction solar cells. Nano Letters, 2009, 9(12): 4250–4257
10. Wang M, Bai J, Le Formal F, Moon S J, Cevey-Ha L, Humphry-Baker R, Grätzel C, Zakeeruddin S M, Grätzel M. Solid-state dye-sensitized solar cells using ordered TiO_2 nanorods on transparent conductive oxide as photoanodes. Journal of Physical Chemistry C, 2012, 116(5): 3266–3273
11. Zhang W, Zhu R, Ke L, Liu X, Liu B, Ramakrishna S. Anatase mesoporous TiO_2 nanofibers with high surface area for solid-state dye-sensitized solar cells. Small, 2010, 6(19): 2176–2182
12. Tétreault N, Horváth E, Moehl T, Brillet J, Smajda R, Bungener S, Cai N, Wang P, Zakeeruddin S M, Forró L, Magrez A, Grätzel M. High-efficiency solid-state dye-sensitized solar cells: fast charge extraction through self-assembled 3D fibrous network of crystalline TiO_2 nanowires. ACS Nano, 2010, 4(12): 7644–7650
13. Wang H, Liu G H, Li X, Xiang P, Ku Z L, Rong Y G, Xu M, Liu L F, Hu M, Yang Y, Han H W. Highly efficient poly(3-hexylthiophene) based monolithic dye-sensitized solar cells with carbon counter electrode. Energy & Environmental Science, 2011, 4 (6): 2025–2029
14. Chen D, Huang F, Cheng Y B, Caruso R A. Mesoporous anatase TiO_2 beads with high surface areas and controllable pore sizes: a superior candidate for high-performance dye-sensitized solar cells. Advanced Materials, 2009, 21(21): 2206–2210
15. Xiang P, Li X, Wang H, Liu G H, Shu T, Zhou Z M, Ku Z L, Rong Y G, Xu M, Liu L F, Hu M, Yang Y, Chen W, Liu T F, Zhang M L, Han H W. Mesoporous nitrogen-doped TiO_2 sphere applied for quasi-solid-state dye-sensitized solar cell. Nanoscale Research Letters, 2011, 6(1): 1–5
16. Tiwana P, Parkinson P, Johnston M B, Snaith H J, Herz L M. Ultrafast terahertz conductivity dynamics in mesoporous TiO_2: influence of dye sensitization and surface treatment in solid-state dye-sensitized solar cells. Journal of Physical Chemistry C, 2010, 114(2): 1365–1371